**Table S1: Related to Figures 1, 5 and 6. Protein constructs**

| Experiment | Expression system | Protein construct description |
|---|---|---|
| *S. cerevisiae* APMS | *S. cerevisiae* | ("Coq9p$^{FLAG"}$) Full length *S. cerevisiae* Coq9p with C-terminal linker (LDLE) and FLAG tag |
| *E. coli* APMS | *E. coli* | ("$His_8$-MBP-tev-$COQ9^{N\Delta 79"}$) Solubility tag ($His_8$-MBP) with linker and TEV protease cleavage site N-terminal to *H. sapiens* COQ9 amino acids 79-318 (N-terminal 79 residues deleted) |
| Crystallography | *E. coli* | ("$COQ9^{N\Delta 79}$" and "$COQ9^{N\Delta 79,C\Delta 31}$ aka $COQ9^{\Delta\alpha 10}$") *H. sapiens* COQ9 amino acid residues 79-218 or 79-287 (C-terminal 31 residues deleted that correspond to the 10$^{th}$ alpha helix) with two additional amino acids residual from TEV protease cleavage |
| Co-purification of COQ7 | Cell-free wheat germ extract | ("SII-$COQ9^{N\Delta 45}$" or "$His_6$-$COQ7^{N\Delta 38}$") N-terminally tagged *H. sapiens* protein with 45 or 38 N-terminal amino acids deleted, respectively |
| *S. cerevisiae* growth | *S. cerevisiae* | ("Coq8p$^{FLAG}$" and "Coq9p$^{FLAG}$") Full length *S. cerevisiae* proteins with C-terminal linker (LDLE) and FLAG tag |

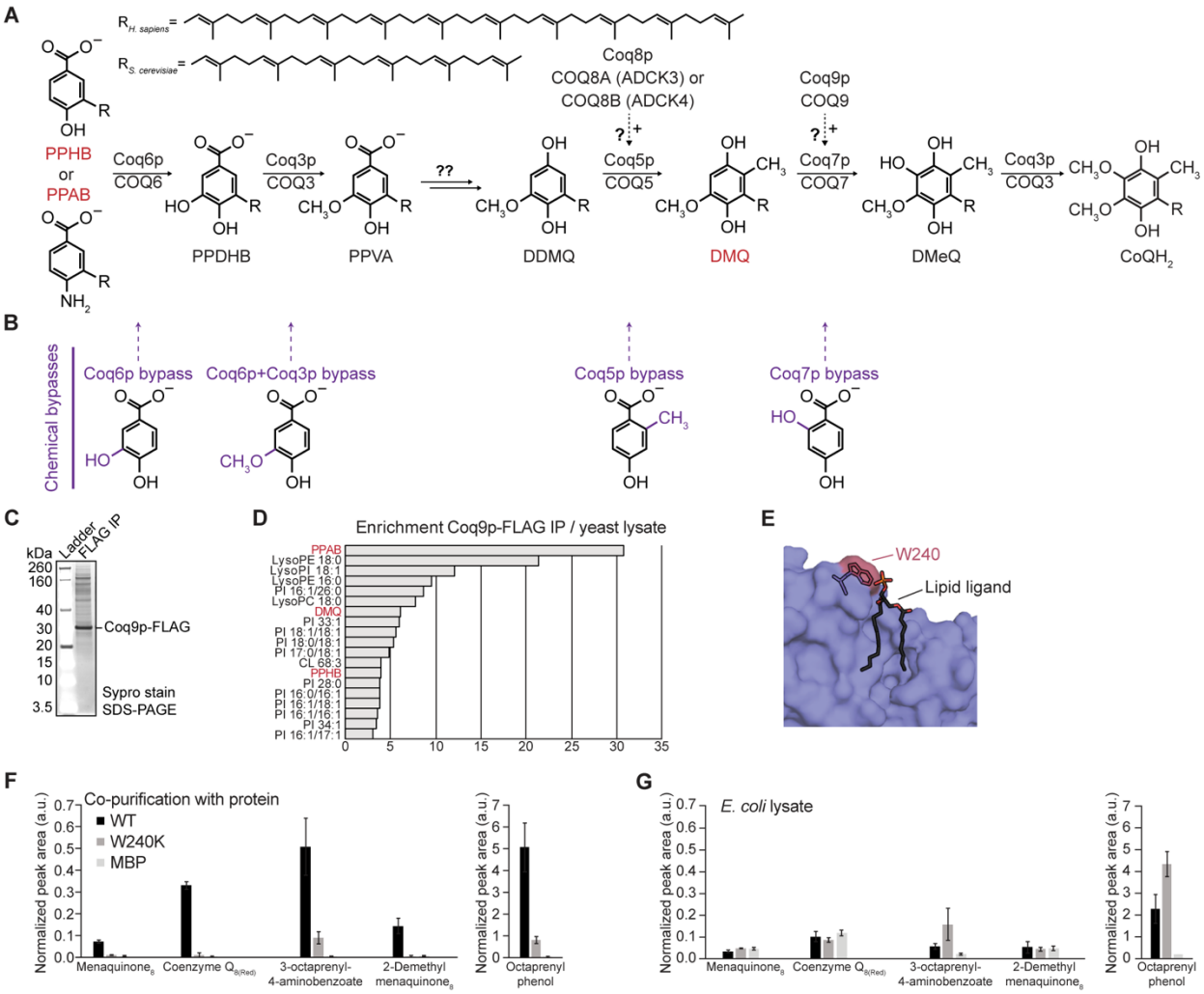


**Figure S1. Related to Figures 1 and 6, LC-MS/MS analysis of COQ9 lipid ligands.**

(A) Head group modifications of eukaryotic CoQ biosynthesis post-attachment of the polyprenyl tail (R) where *S. cerevisiae* (Coq#p) and *H. sapiens* (COQ#) protein names are shown. PPHB, polyprenyl-hydroxybenzoate; PPAB, polyprenyl-aminobenzoate; PPDHB, polyprenyl-dihydroxybenzoate; PPVA, polyprenyl-vanillic acid; DDMQ, demethoxy-demethyl CoQ; DMQ, demethoxy CoQ; DMeQ, demethyl CoQ; $CoQH_2$, reduced CoQ.

(B) Chemical head group bypasses used in Figures 6 and S6, where pre-modified moieties are in purple.

(C) Sypro-stained SDS-PAGE of Coq9p-FLAG immuno-purification from *S. cerevisiae.*

(D) Top ranking identified lipids enriched (enrichment > 3, *p*-value < 0.05) in Coq9p-FLAG pull-down from *S. cerevisiae* compared to whole cell lysate (Spreadsheet S2). CoQ intermediates are highlighted in red in panels A and D.

(E) Co-crystallized phospholipid with COQ9, where W240 is in red and the phospholipid is in black stick, PDB ID 4RHP.
(F) LC-MS/MS quantification of enriched *E. coli* lipids from purified protein in Fig. 1, where WT is $His_8$-MBP-$COQ9^{N\Delta79}$, W240K is $His_8$-MBP-$COQ9^{N\Delta79,\ W240K}$ and MBP is $His_6$-MBP. Lipid peak areas are normalized to the total peak area per sample and error bars represent standard deviation (n=3, Spreadsheet S2).
(G) LC-MS/MS quantification of *E. coli* lipids in Fig. 1 from the *E. coli* lysates expressing recombinant protein, with bar colors described in panel F: WT is $His_8$-MBP-$COQ9^{N\Delta79}$, W240K is $His_8$-MBP-$COQ9^{N\Delta79,\ W240K}$ and MBP is $His_6$-MBP. Lipid peak areas are normalized to the total peak area per sample and error bars represent standard deviation (n=3, Spreadsheet S2).

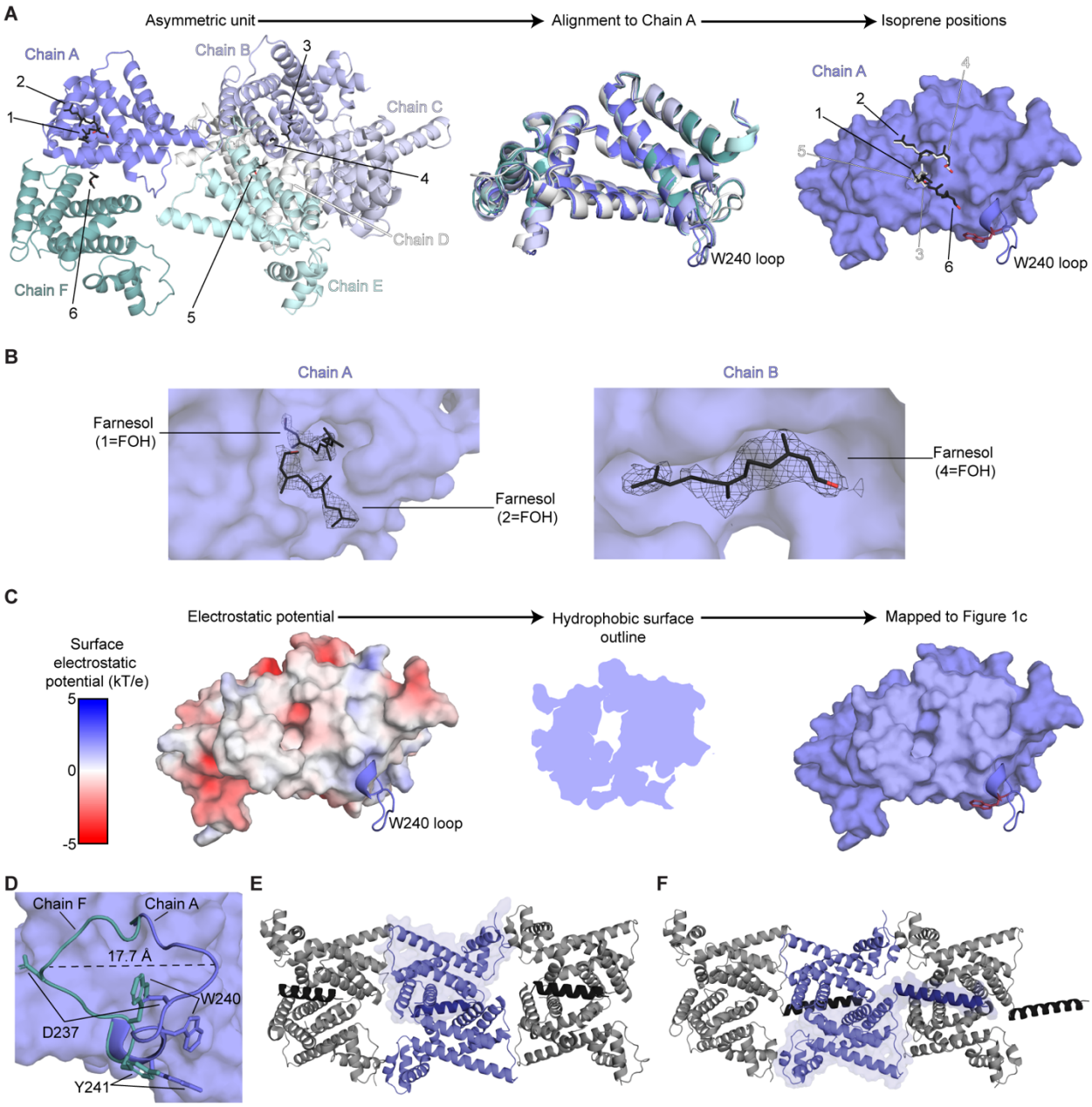


**Figure S2. Related to Figures 1 and 2, Crystal structure of COQ9 with geranylgeraniol and extended helix 10.**

(A) Six modeled isoprene positions (black, #1-6) on six COQ9 chains (A-F) in the asymmetric unit (PDB: 6DEW), where Chains A-F are in blue, light blue, blue-white, white, light cyan, and light teal respectively. All chains and co-crystallizing isoprenes were then aligned to Chain A. Isoprene positions shown in Fig. 1 are in black and those co-crystallizing in similar positions are in white.

(B) Composite simulated annealing omit maps showing electron density (1$\sigma$) for the most ordered isoprenes (FOH ligands in Chains A and B). Similar electron density that was somewhat less well defined was observed at the same sites in all of the protomers.
(C) Electrostatic potential of COQ9 Chain A generated by the Adaptive Poisson-Boltzmann Solver (Jurrus et al., 2018). The $\alpha$7-$\alpha$8 loop is excluded from the surface. Negative electrostatic potential is red, positive is blue, and zero is white. The hydrophobic surface was outlined and mapped to Figure 1C.
(D) Overlay of COQ9$^{N\Delta79,C\Delta31}$ chains A (blue) and F (teal), where conformations of the $\alpha$7-$\alpha$8 loop are in cartoon and COQ9 residues important for COQ7 binding (D237, W240, Y241) are highlighted. The difference between loop conformations is 17.7 Å, at its widest point (dotted line).
(E) Modeled position of $\alpha$10 in the original COQ9 structure (PDB: 4RHP) where the $\alpha$9-$\alpha$10 loop was not resolved. Symmetry mates are in gray, a single COQ9 protomer is outlined in surface, and $\alpha$10 is in either dark blue or black.
(F) Position of $\alpha$10 in the structure reported in this work (PDB: 6AWL) where the $\alpha$9-$\alpha$10 loop was resolved and shows that $\alpha$10 extends away from globular COQ9 to form crystal contacts with an adjacent COQ9 molecule. Symmetry mates are in gray, a single COQ9 protomer is outlined in surface, and $\alpha$10 is in either dark blue or black.

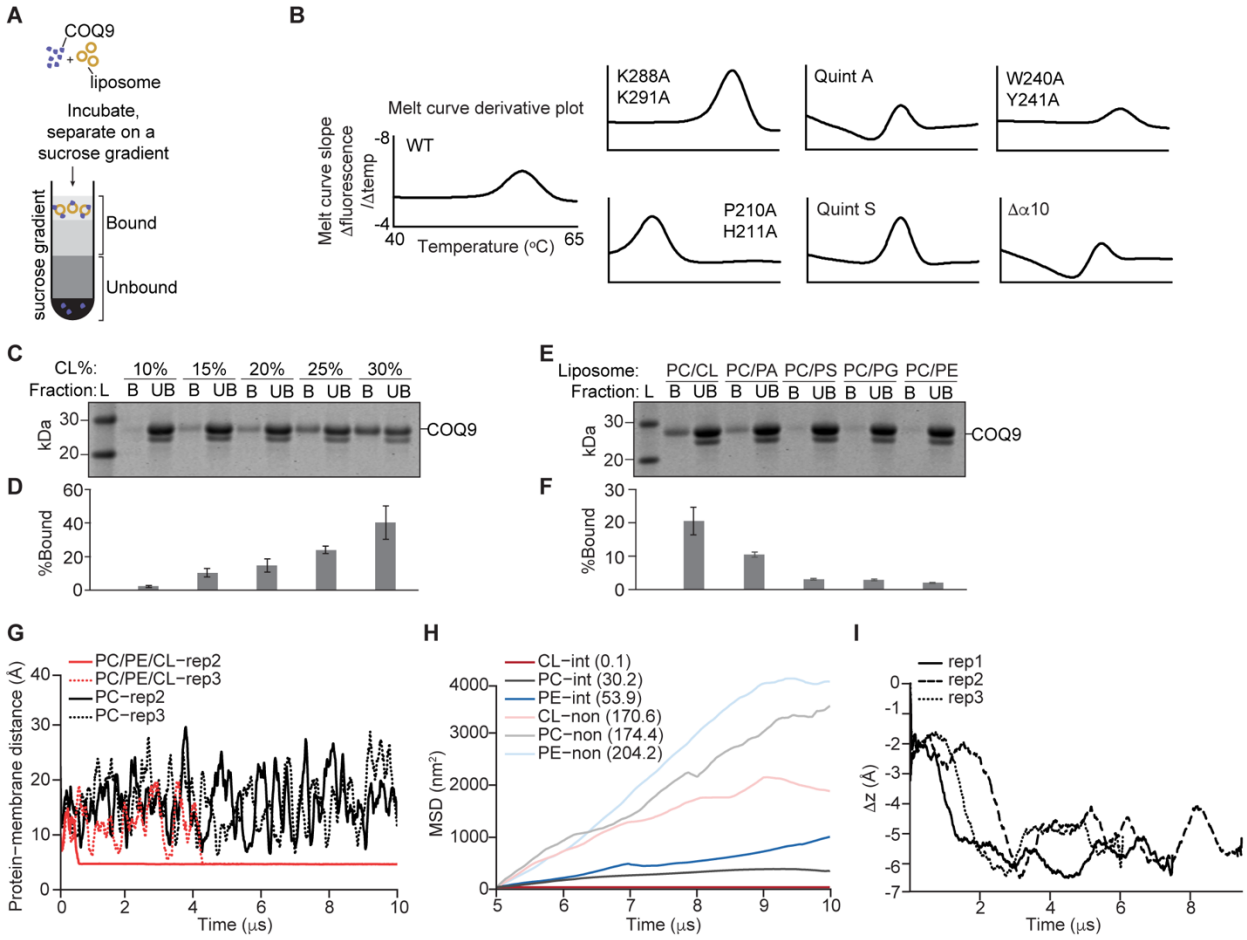


**Figure S3. Related to Figures 3 and 4, COQ9 liposome binding *in vitro* and membrane binding *in silico*.**

(A) Liposome co-flotation schematic where liposome bound (B) and unbound (UB) fractions quantified by SDS-PAGE densitometry are shown.

(B) Thermal melt curve derivative plots (Δfluorescence/Δtemperature from 40–65 °C) for proteins assayed by liposome co-flotation as measured by differential scanning fluorimetry. All plots are scaled as shown in WT and the thermal melting temperature ($T_m$) is at the apex of the melt curve derivative plot.

(C) SDS-PAGE of liposome co-flotation of $COQ9^{N\Delta 79}$ with PC/CL/NBD-PE liposomes, with increasing CL molar % (10,15,20,25,30) where NBD-PE is at a constant 0.1 molar %, as described in Figure 3.

(D) Quantification of liposome bound COQ9 in panel C by densitometry (100×B/Total) where error bars represent standard deviation (n=2).

(E) SDS-PAGE of liposome co-flotation of $COQ9^{N\Delta 79}$ in PC/CL/NBD-PE, PC/PA/NBD-PE, PC/PS/NBD-PE, PC/PG/NBD-PE, or PC/PE/NBD-PE (all 77.9/22/0.1 molar %) liposomes.

(F) Quantification of liposome bound COQ9 in panel E by densitometry (100×B/Total) where error bars represent standard deviation (n=2).
(G) Time evolution of the minimum pairwise distance between COQ9 and the membrane (PC (black) or PC/PE/CL (red)) in CG-MD simulation replicas 2 (solid) and 3 (dotted).
(H) Mean square displacement of representative CL (red), PC (gray), PE (blue) lipids, for those that establish a stable interaction with COQ9 ("int," dark colors) and never interact with COQ9 ("non," light colors) for a PC/PE/CL membrane (replica 1). Lateral diffusion coefficients are given in $nm^2/\mu s$ in parentheses in the legend for replica 1. Lateral diffusion coefficients in $nm^2/\mu s$ for replica 2: CL-int: 0.4, PC-int: 22.4, PE-int: 7.5, CL-non: 90.5, PC-non: 157.6, PE-non: 136.5, and for replica 3: CL-int: 2.3, PC-int: 9.1, PE-int: 7.2, CL-non: 112.3, PC-non: 131.0, PE-non: 123.9.
(I) The z-shift of lipid phosphate head groups that are within 12 Å of membrane-bound COQ9 relative to the base plane of membrane lipid phosphate head groups, for replicas 1 (solid), 2 (dashed), and 3 (dotted). For each replica, t=0 μs refers to the beginning of a stable interaction of the protein with the membrane (Step 4 in Fig. 3A); therefore, each replica has a different total membrane interaction time.

A

| COQ9 Residues | | | COQ7 Residues | | |
|---|---|---|---|---|---|
| Residue | COQ7 binding when mutated | Constrained in docking | Residues | COQ9 binding when mutated | Constrained in docking |
| W240 | No | Yes:Interacting | W115 | No | Yes: Interacting |
| Y241 | No | Yes:Interacting | R105 | No | Yes: Interacting |
| D237 | Diminished | Yes:Interacting | I203 | No, but not possible to model in structure | No |
| R244 | Diminished | No | P108 | No | Yes: Interacting |
| L256 | Diminished, but less thermally stable | No | L111 | No | Yes: Interacting |
| L190 | Diminished, but not thermally stable | No | S214 | Diminished, but not possible to model in structure | No |
| M227 | Diminished, but not thermally stable | No | R154 | Yes | Yes:Not interacting |
| S131 | Yes | Yes:Not interacting | Q89 | Yes | Yes:Not interacting |
| D261 | Yes | Yes:Not interacting | E143 | Yes | Yes:Not interacting |
| A287-R318 (α10) | Yes | Yes:Not interacting | R175 | Yes | Yes:Not interacting |
| | | | D183 | Yes | Yes:Not interacting |
| | | | Y196 | Yes | Yes:Not interacting |

B

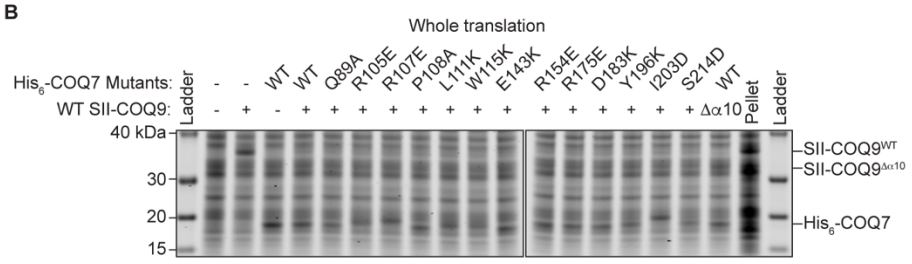


C

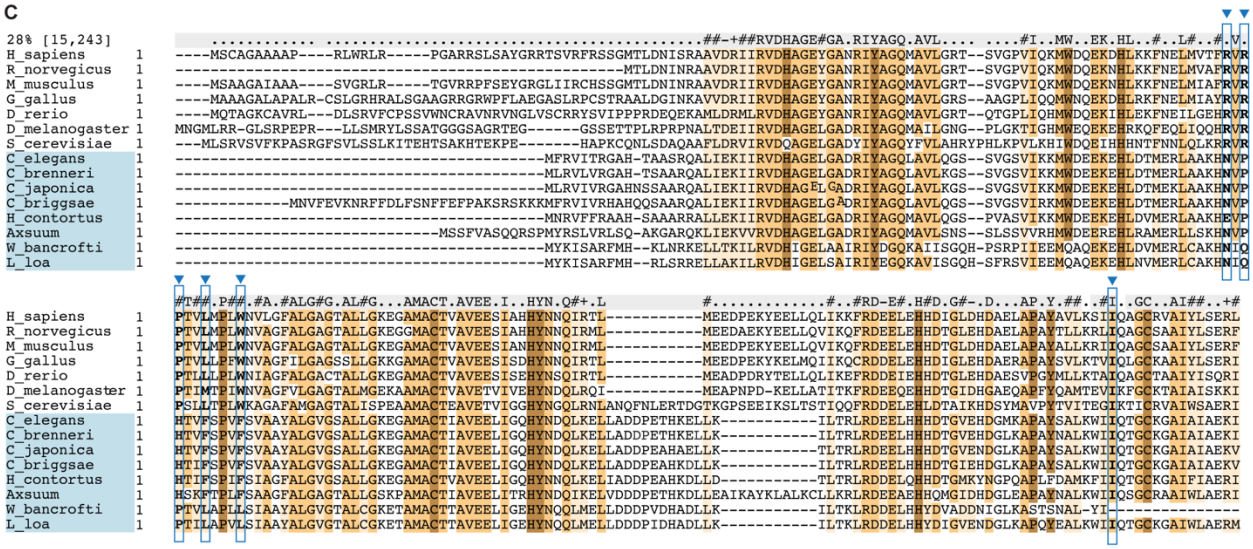


**Figure S4. Related to Figure 5, COQ9 and COQ7 protein interactions.**

(A) Mutants tested in COQ9:COQ7 reactions (from this work, see Figure 5 and Lohman *et al.* (Lohman et al., 2014)) and their incorporation as constraints for molecular docking.

(B) Protein translations in cell-free wheat germ extract from which SII-COQ9$^{N\Delta 45}$ in Figure 5A was purified.

(C) Multiple sequence alignment of COQ7 with conserved residues in orange, residues important for the COQ9 interaction outlined in blue, and species lacking COQ9 homologues highlighted in blue.

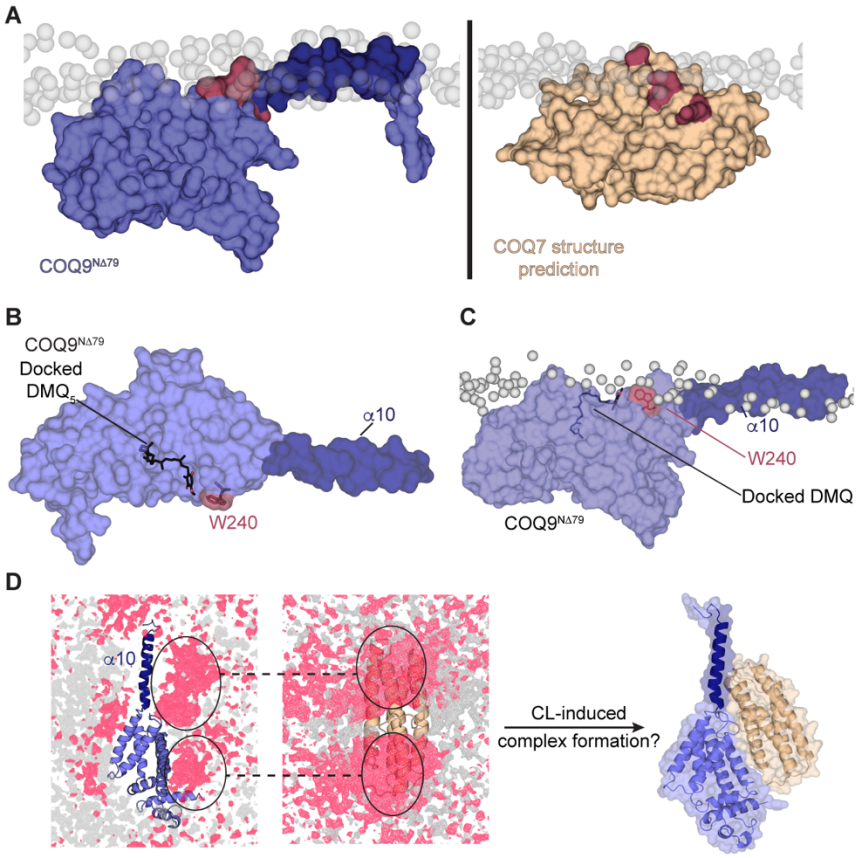


**Figure S5. Related to Figure 5, COQ9 and COQ7 docking.**

(A) Membrane binding CG-MD simulations of COQ9 and COQ7 with protein-protein interface residues in red.

(B) Molecular docking of $DMQ_5$ (stick) on $COQ9^{N\Delta79}$ (PDB: 6AWL, Chain A) where $\alpha$10 (dark blue) and W240 (red) are labeled.

(C) Molecular docking of $DMQ_5$ (stick) superimposed on the membrane-bound conformation of $COQ9^{N\Delta79}$ where W240 is shown in red, membrane phospholipid head groups in gray, and $\alpha$10 in dark blue.

(D) Occupancy of lipid phosphate head groups in CG-MD simulations of COQ9 (left) and COQ7 (middle) with CL in red and PC/PE in gray, where CL-rich regions are circled and COQ9 and COQ7 are oriented as in the modeled COQ9:COQ7 complex (right and Figure 5).

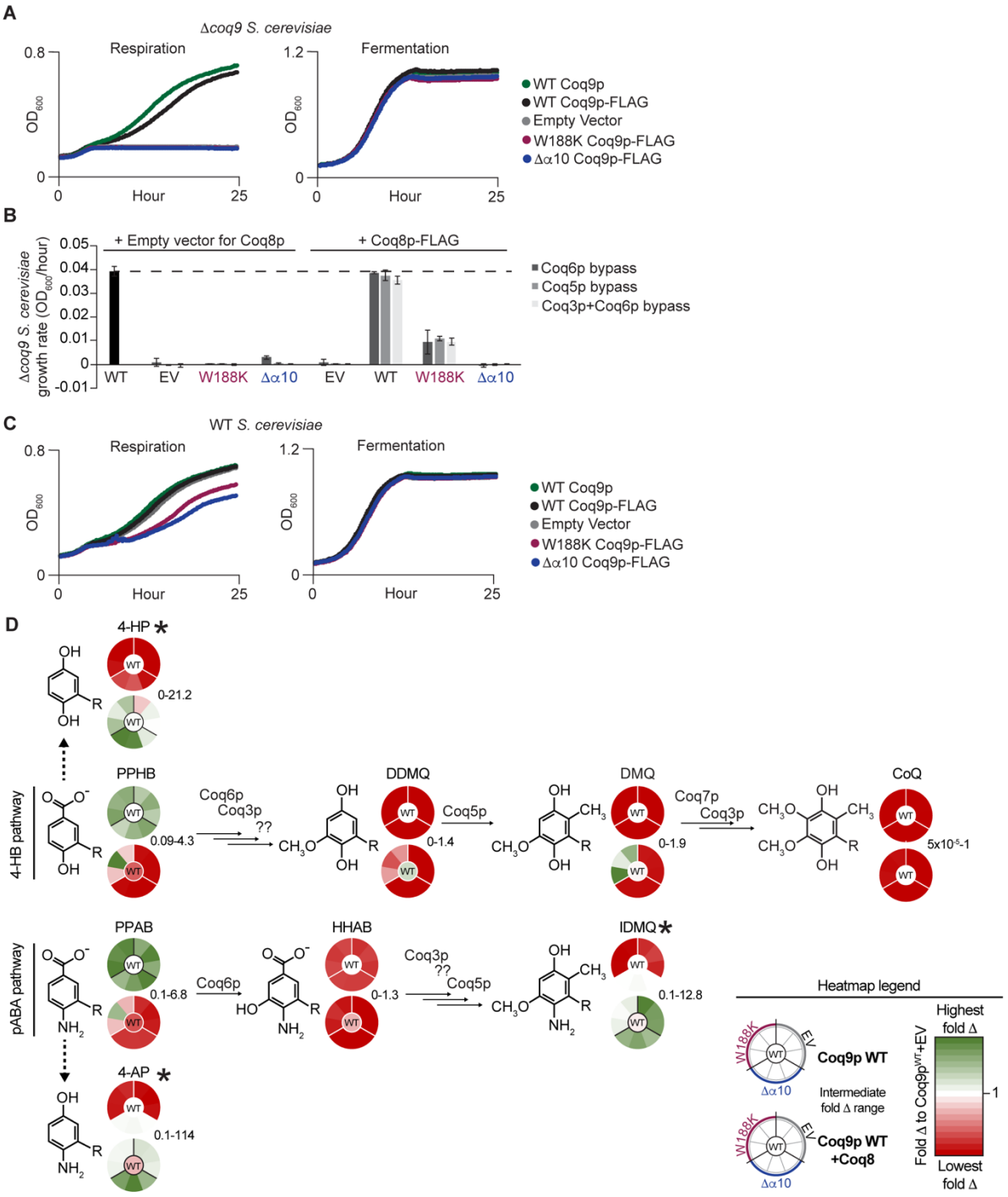


**Figure S6. Related to Figure 6, Coq9p mutant growth inhibition profile.**

(A) Growth curves of Δ*coq9 S. cerevisiae* overexpressing Coq9p mutants in respiration (CoQ-dependent) and fermentation (CoQ-independent) conditions.

(B) Respiration growth rates ($OD_{600}$/hr post-diauxic shift) of Δ*coq9 S. cerevisiae* overexpressing Coq9p-FLAG mutants and combinations of Coq8p-FLAG, empty vector, and chemical bypasses for Coq6p, Coq5p, and Coq3p+Coq6p (see Figure S1). Overexpressed WT Coq9p-FLAG (black

bar) is a reference for complete rescue (dotted line) and EV refers to empty vector for Coq9p expression (p416GPD). Error bars represent standard deviations of growth rates (n=3).
(C) Growth curves of WT *S. cerevisiae* overexpressing Coq9p mutants, as described in panel A.
(D) *S. cerevisiae* CoQ intermediates in Coq9p mutants. Levels of CoQ intermediates in Δ*coq9* yeast overexpressing either $Coq9p^{WT}$, empty vector (EV), $Coq9p^{\Delta\alpha 10}$, or $Coq9p^{W188K}$ with and without Coq8p-FLAG co-expressed (n=3). Heat maps correspond to individual intermediate levels relative to Δ*coq9* + $Coq9p^{WT}$ + EV (white) without Coq8p, where red shows a decrease, green shows an increase, and the layout for each heatmap is shown in the legend. Intermediates associated with Coq6p defects (4-HP, 4-AP, and IDMQ) are annotated with an asterisk.

A

| Helix Swap | Species | AA residues | Key Features |
|---|---|---|---|
| Kes1p | *S.c.* | 7-29 | Binds to + curvature |
| VLCAD | *H.s.* | 482-514 | Binds to CL and IMM |
| Opi1p | *S.c.* | 111-128 | Binds to PA |
| Coq8p | *S.c.* | 74-94 | Inserts into IMM |

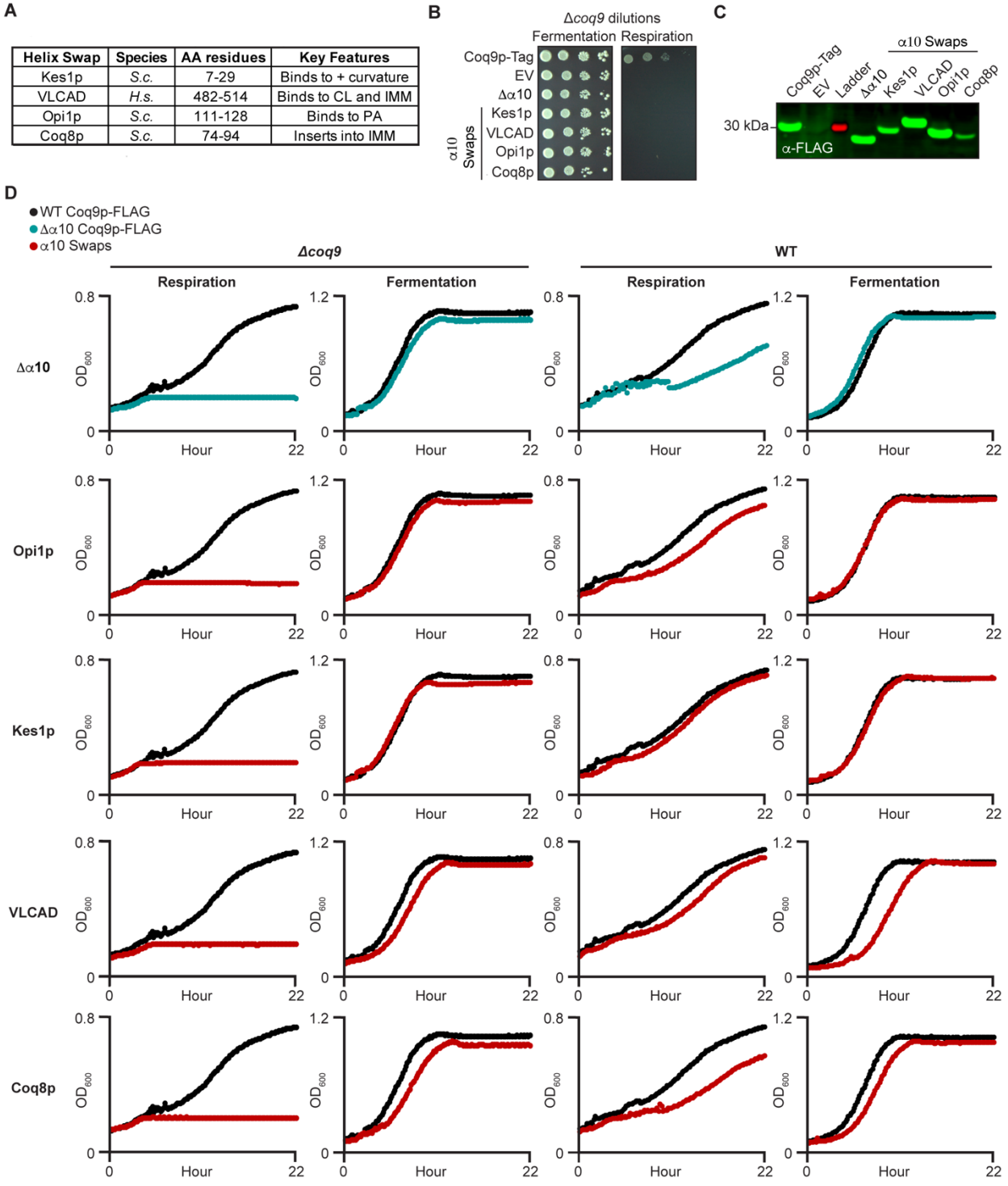


**Figure S7. Related to Figure 6, Phenotypes of α10 swap chimeric proteins.**

(A) Table of amphipathic and transmembrane helix swaps: Kes1p (Drin et al., 2007), VLCAD (McAndrew et al., 2008) (Zhang et al., 2015), Opi1p (Hofbauer et al., 2018), Coq8p (Reidenbach et al., 2018) (Xie et al., 2011).

(B) Drop assay of Δ*coq9* yeast expressing helix swap chimeras or controls (WT Coq9p$^{FLAG}$, empty vector, Δα10 Coq9p$^{FLAG}$) on fermentation or respiration media.
(C) Western blot (anti-FLAG) of whole cell WT yeast containing FLAG-tagged helix swap constructs.
(D) Representative growth curves for helix swap chimeras (red dots) expressed in Δ*coq9* or WT yeast, in fermentation or respiration media. WT Coq9p$^{FLAG}$ curves are shown in black dots, α10 Coq9p$^{FLAG}$ in teal dots.